2636 *Biochemistry* **2010,** *49,* 2636–2646
DOI: 10.1021/bi902082d

BIOCHEMISTRY
including biophysical chemistry & molecular biology
Article

Cold Adaptation in DEAD-Box Proteins[†]

Gwendoline Cartier, Florence Lorieux,[‡] Frédéric Allemand, Marc Dreyfus,* and Thierry Bizebard*

CNRS UPR9073, University Paris VII, Institut de Biologie Physico-chimique, 13 rue Pierre et Marie Curie, 75005 Paris, France. [‡]Present address: Institut de Génétique et Microbiologie, Université Paris-Sud, CNRS UMR8621, Bât. 400, 91405 Orsay Cedex, France.

Received December 8, 2009; Revised Manuscript Received February 12, 2010

ABSTRACT: Spontaneous rearrangements of RNA structures are usually characterized by large activation energies and thus become very slow at low temperatures, yet RNA structure must remain dynamic even in cold-adapted (psychrophilic) organisms. DEAD-box proteins constitute a ubiquitous family of RNA-dependent ATPases that can often unwind short RNA duplexes in vitro (helicase activity), hence the belief that one of their major (though not exclusive) roles in vivo is to assist in RNA rearrangements. Here, we compare two *Escherichia coli* DEAD-box proteins and their orthologs from the psychrophilic bacteria *Pseudoalteromonas haloplanktis* and *Colwellia psychrerythraea* from the point of view of enzymatic properties. One of these proteins (SrmB) is involved in ribosome assembly, whereas the other (RhlE) presumably participates in both mRNA degradation and ribosome assembly; in vitro, RhlE is far more active as a helicase than SrmB. The activation energy associated with the ATPase activity of the psychrophilic SrmB is lower than for its mesophilic counterpart, making it more active at low temperatures. In contrast, in the case of psychrophilic RhlE, it is the RNA unwinding activity, not the ATPase activity, that has a reduced activation energy and is therefore cold-adapted. We argue that these different modes of cold adaptation reflect the likely function of these proteins in vivo: RNA helicase for RhlE and ATP-dependent RNA binding for SrmB. The cold adaptation of helicases like RhlE presumably facilitates RNA metabolism in psychrophilic bacteria.

Temperature is one of the main physical parameters to which living organisms have adapted. For instance, bacteria can grow in the entire range of temperatures where water remains liquid (from ca. −15 to 110 °C). Remarkably, many cold-adapted (psychrophilic) bacteria grow at 0−10 °C almost as fast as their mesophillic cousins at higher temperatures, despite the slowing of all chemical reactions in the cold (*1*, *2*). One way psychrophilic organisms may cope with this slowing is to increase the concentration of their enzymes, a strategy with obvious limits, or to improve their catalytic efficiency. Indeed, many studies have shown that enzymes of psychrophilic origin are endowed with lower activation enthalpies ($\Delta H^{\ddagger}$) than their mesophilic counterparts, which make them better catalysts in the cold (for reviews, see refs (*3*−*5*)).

Among all reactions that psychrophilic organisms need to keep fast at low temperature stands the rearrangement of RNA or ribonucleoprotein (RNP) structures. Many RNA molecules need to undergo rapid structural rearrangements in vivo, either because their normal function implies that they transiently form intra- or intermolecular duplexes (*6*) or because they occasionally get trapped into misfolded structures that must be resolved (*7*). Keeping these rearrangements fast at low temperatures constitutes a major challenge. Indeed, the stability of RNA duplexes is a compromise between enthalpic and entropic contributions that, beyond a few base pairs in length, become very large. Therefore, as a consequence of the van't Hoff and Arrhenius laws, even duplexes that are only marginally stable at room temperature can become extremely stable and long-lived around 0 °C (*8*, *9*) (see Figure 6). In vivo, it is believed that rearrangements of RNA structures are assisted by specialized proteins. Among them stand DEAD-box proteins, which constitute a ubiquitous family of RNA-dependent ATPases and ATP-dependent RNA binding proteins characterized by nine conserved motifs, including the eponymous D-E-A-D motif (*10*). They are essential to nearly all reactions involving RNA in vivo, particularly in eukaryotes (*10*). In vitro, many of them can unwind short (< 20 bp) RNA duplexes. On this basis, it is often assumed that in vivo DEAD-box proteins serve to facilitate local structural rearrangements in RNA molecules (*11*). In some cases, this "RNA chaperone" role has clearly been documented (*7*, *12*, *13*). However, it is becoming increasingly clear that not all DEAD-box proteins serve to unwind RNA duplexes in vivo: some of them appear to displace proteins from ribonucleoprotein complexes (*14*, *15*), whereas others simply bind particular RNAs in an ATP-dependent manner (*16*).

Escherichia coli possess five DEAD-box proteins, named SrmB, CsdA (also called DeaD), DbpA, RhlB, and RhlE (reviewed in ref *17*). All these proteins have RNA-dependent ATPase and RNA helicase activities in vitro (*18*−*20*). In vivo, they participate in at least two fundamental cellular processes, i.e., mRNA degradation (*21*−*25*) and ribosome assembly (*26*−*31*). Both processes require that RNA adopt a particular conformation (single-stranded structure for mRNA degradation and native rRNA structure for ribosome assembly) that may be

[†]This work was supported by Centre National de la Recherche Scientifique (CNRS), by Ecole Normale Supérieure, and by the Agence Nationale de la Recherche [Grants NT05-1_44659 (CARMa) and 08-BLAN-0086-02 (mRNases) to M.D.].

*To whom correspondence should be addressed. T.B.: telephone, (33) 1 58 41 52 36; fax, (33) 1 58 41 50 20; e-mail, Thierry.Bizebard@ibpc.fr. M.D.: telephone, (33) 1 58 41 51 22; fax, (33)1 58 41 50 20; e-mail, marc.dreyfus@ibpc.fr.

 Published on Web 02/18/2010

favored by DEAD-box proteins. Of note, whereas all five DEAD-box proteins are dispensable at 37 °C, two of them (SrmB and CsdA) become essential at lower temperatures [20 °C (see Figure 3A,B)], and at least one of them (CsdA) is overexpressed under these conditions (*32*). Presumably, at 37 °C, enough thermal energy is available for the spontaneous population of the conformations that are favored by SrmB and CsdA, but at 20 °C, this energy becomes scarce. Growth then becomes dependent upon these proteins, more so as the temperature decreases. Interestingly, overexpression of DEAD-box proteins at low temperatures has also been observed in other microorganisms (*33*), including psychrophilic ones (*34*).

An intriguing question is whether, besides being overexpressed, DEAD-box proteins from psychrophilic organisms have evolved special properties to cope with very low temperatures. To address this question, we have compared the enzymatic properties of orthologous DEAD-box proteins from *E. coli* and from two of its cold-adapted relatives, the marine γ-proteobacteria *Pseudoalteromonas haloplanktis* (*35*) and *Colwellia psychrerythraea* (*36*). Two of the five *E. coli* proteins, RhlE and SrmB, were selected for this study because they stand among the most and least active in helicase assays in vitro, respectively (*17*, *19*). Our results show that psychrophilic RhlE and SrmB have indeed adapted to low temperatures, but that the enzymatic parameters that have been adapted differ in both cases, presumably reflecting the different functions of these two proteins in vivo.

EXPERIMENTAL PROCEDURES

Growth of Cells. *P. haloplanktis* TAC125 (a gift from A. Danchin) and *C. psychrerythraea* 34H (ATCC reference BAA-681) were grown aerobically in Difco Marine broth 2216, a salty rich medium that can also be used for *E. coli*. Whereas the growth of *E. coli*, which is maximal at 39 °C, becomes very slow around 10 °C and undetectable below 8 °C, both *P. haloplanktis* and *C. psychrerythraea* grew readily in the cold (doubling time of ca. 12 h at 0 °C). *P. haloplanktis* grew over a broad temperature range, with optimal and maximal growth temperatures of ca. 26 and 32 °C, respectively. In contrast, *C. psychrerythraea* is a stricter psychrophile, with a reported optimal growth temperature of 8 °C (*36*), and no growth was observed above 20 °C. The mesophilic or psychrophilic character of the three organisms can be readily visualized by plating them at different temperatures (Figure S1 of the Supporting Information). For genomic DNA extraction, *P. haloplanktis* and *C. psychrerythraea* were grown at 12 °C (doubling times of 1.75 and 2.5 h, respectively), and DNA was extracted as described in ref *37*.

Cloning, Overexpression, and Purification of Proteins. To identify orthologs of the *E. coli* DEAD-box proteins SrmB and RhlE in *P. haloplanktis* TAC125 and *C. psychrerythraea* 34H, BLAST-P with default settings was used, except that no low complexity filter was included (www.ncbi.nlm.nih.gov). This analysis identified putative orthologs of SrmB and RhlE in *P. haloplanktis* (NCBI accession numbers YP_339043 and YP_340437, respectively) and in *C. psychrerythraea* (NCBI accession numbers YP_270752 and YP_267868, respectively). The sequences of the orthologs were visually aligned with those of the corresponding *E. coli* proteins for unambiguous assignment of the start codon. In the following, the name of each DEAD-box protein is followed by _Ec (*E. coli*), _Ph (*P. halopkanktis*), or _Cp (*C. psychrerythraea*) to indicate its origin.

The ORFs[1] of SrmB_Ph, SrmB_Cp, RhlE_Ph, and RhlE_Cp were amplified by PCR from the corresponding genomic DNA using the F (forward) and R (reverse) primers listed in Table S1 (Supporting Information). PCR products were digested at the restriction sites italicized in Table S1 and ligated into the same sites of the pPROEX-HTa expression vector (Invitrogen). For protein purification, *E. coli* BL21(DE3) cells transformed with the corresponding pPROEX-HTa derivatives were grown at 37 °C to an OD_{600} of 0.5−1.0 in LB or in tryptone-phosphate broth (*38*) supplemented with 0.01% ampicillin and then induced overnight at 12−16 °C with 0.5 mM IPTG. Purification of the four proteins, as well as SrmB_Ec and RhlE_Ec, was conducted as described in ref *19*, except that commercial TEV protease (Invitrogen) was used. All proteins were dialyzed versus storage buffer [20 mM Hepes-Na (pH 7.5), 300 mM NaCl, 20% (v:v) glycerol, 0.1 mM EDTA, and 1 mM DTT] and quantified from their OD_{280} values using extinction coefficients computed with ProtParam (www.expasy.ch). After homogeneity had been checked by denaturing gel electrophoresis, proteins were aliquoted, flash-frozen, and stored at −80 °C.

Complementation Assays. For complementation studies, the *srmB_Ph* gene with 500 and 700 nt of upstream and downstream sequence, respectively, was amplified from the *P. haloplanktis* DNA using oligonucleotides SrmB_Ph F1 and SrmB_Ph R1 (Table S1 of the Supporting Information). Similarly, the *srmB_Cp* gene with 350 and 25 nt of upstream and downstream sequence, respectively, was amplified from the *C. psychrerythraea* DNA with oligonucleotides SrmB_Cp F1 and SrmB_Cp R1. The fragments were cloned into the EcoRI site (after Klenow filling in the case of SrmB_Ph) of low-copy number plasmid pCL1920 (*39*) and introduced into ENS133ΔSrmB, an *E. coli* strain lacking SrmB (*26*). For control, ENS133ΔsrmB and the parent strain ENS133 (*40*) were also transformed with pCL1920. The growth of these different strains was then compared at 20 °C on plates on which aliquots (3 μL) of serially diluted saturated cultures had been deposited. Polysome profiles (30 °C) were analyzed as described in ref *26*.

To test the functionality of RhlE_Ph and RhlE_Cp, pPROEX-HTa derivatives carrying the *csdA*, *rhlE_Ec*, *rhlE_Ph*, or *rhlE_Cp* gene were introduced into ENS133ΔCsdA, an ENS133 derivative constructed from WJW45ΔCsdA (*27*) by P1 transduction. The parent plasmid was also used as a control. Cell growth was recorded as described above, using plates containing suboptimal IPTG concentrations (from 0 to 20 μM) to limit the expression of the cloned genes. Polysome profiles (25 °C) were determined as described above, except that cells were induced with 200 μM IPTG for 30−60 min before being harvested.

ATPase Assays. ATPase activities were assayed by enzymatically coupling ATP hydrolysis to NADH oxidation (*19*). The latter was recorded versus time at 340 nm using a Uvikon 930 spectrophotometer (Kontron) equipped with a thermostated cell holder, assuming an ε_{340} of 6220 M^{-1} cm^{-1} for NADH. Blanks without DEAD-box proteins were subtracted from the measurements. Averaged data from at least two independent experiments were analyzed with KaleidaGraph (Synergy Software). Assays were conducted in 10 mM Hepes-Na (pH 7.5), 60 mM NaCl, 55 mM KCl, 5% (v:v) glycerol, and, unless otherwise stated,

[1]Abbreviations: IPTG, isopropyl β-D-1-thiogalactopyranoside; ORF, open reading frame; TEV, tobacco etch virus; AMP-PNP, 5′-adenylyl-imido-diphosphate; nt, nucleotides; poly(A), polyadenylic acid; poly(U), polyuridylic acid.

2 mM ATP/Mg (a stoichiometric mix of ATP and $MgCl_2$). Both poly(A) (Sigma) and a duplex used for the helicase assay (see below) were used as RNA activators. The concentrations of the two coupling enzymes, pyruvate kinase and lactate dehydrogenase (Roche), were such that, at all temperatures tested, their activities exceeded at least 100-fold the assayed ATPase activity (> 5 units/mL vs < 0.05 unit/mL; one unit corresponds to 1 μmol of substrate reacting per minute). That ATPase activity is rate-limiting in the assay even at low temperatures (5 and 10 °C) was confirmed by checking that the reaction rate was proportional to DEAD-box protein concentration.

RNA Substrates for Helicase Assays. RNA oligoribonucleotides (Eurogentec) were resuspended in 10 mM MOPS-Na (pH 7.0). Their concentration was estimated from their OD_{260} using extinction coefficients provided by the manufacturer. Their sequences are as follows: Cy5-labeled 9-mer, Cy5-5′-GCUUU-ACGG-3′; Cy5-labeled 10-mer, Cy5-5′-GCUUUACGGU-3′; Cy5-labeled 11-mer, Cy5-5′-GCUUUACGGUG-3′; Cy3-labeled 26-mer, 5′-AACAAAACAAAAUAGCACCGUAAAGC-3′-Cy3; unlabeled 14-mer, 5′-UAGCACCGUAAAGC-3′.

These oligonucleotides are derived from those used in ref *19*; they are designed to minimize intramolecular structures. Duplexes between the Cy3 26-mer and the Cy5 9-, 10-, and 11-mers were prepared via incubation of equimolar amounts (10−20 μM) of complementary oligonucleotides for 10 min in 75 mM KCl and 10 mM Hepes-Na (pH 7.5) at room temperature. Duplex formation brings the two fluorophores (the donor Cy3 and the acceptor Cy5) into the proximity of one another, allowing fluorescence resonance energy transfer (FRET) between them.

Continuous Helicase Assays. Unwinding rates were measured between 1 and 37 °C, using 50 μL quartz microcuvettes and a Varian Eclipse spectrofluorimeter equipped with a temperature controller. Assays were performed in the same buffer as ATPase assays, routinely containing 20 nM fluorescent duplex, 0.2 μM unlabeled 14-mer, and 2 mM ATP/Mg or the nonhydrolyzable analogue AMP-PNP/Mg. The DEAD-box protein (0.6−0.8 μM) was added last to start the reaction. The fluorescence of the donor (Cy3) was measured versus time with excitation at 500 nm and emission at 565 nm, whereas FRET from Cy3 to Cy5 was measured with excitation at 540 nm and emission at 665 nm. In both cases, 10 nm slit widths were used.

All unwinding assays were conducted at least in duplicate, in parallel with samples lacking either DEAD-box protein or ATP (or containing 2 mM AMP-PNP). In most cases (but see below), the fluorescence of samples without protein remained stable with time (Figure 1B), indicating that both photobleaching and spontaneous duplex dissociation were negligible. In the presence of DEAD-box protein, but without ATP, fluorescence variations also remained very limited, and no kinetic end points could be reached. In contrast, in the presence of both DEAD-box protein and ATP, duplex unwinding is readily observed, as shown by the increase in donor fluorescence and decrease in FRET (Figure 1B). We estimate that, in all cases tested, unwinding is at least 50 times faster in the presence of ATP than in its absence.

The time course of the donor fluorescence (F) and FRET signals were nonlinearly fitted to the equations $F(t) = F_0 + (F_\infty - F_0)[1 - \exp(-k_{unw}t)]$ and $FRET(t) = FRET_\infty + (FRET_0 - FRET_\infty)\exp(-k'_{unw}t)$, respectively, using KaleidaGraph (first-order kinetics). Correlation coefficients (R) were always above 0.99. Moreover, the two rate constants, k_{unw} and k'_{unw}, were always within 15% of each other. In a limited number of cases, F and FRET did not reach a plateau but decreased linearly with time, due presumably to photobleaching. In this case, the equations were modified to $F(t) = F_0 + (F_\infty - F_0)[1 - \exp(-k_{unw}t)] - k_{bleach}t$ and $FRET(t) = FRET_\infty + (FRET_0 - FRET_\infty)\exp(-k'_{unw}t) - k'_{bleach}t$. With this correction, the values obtained for k_{unw} and k'_{unw} remained very similar (to ±20%).

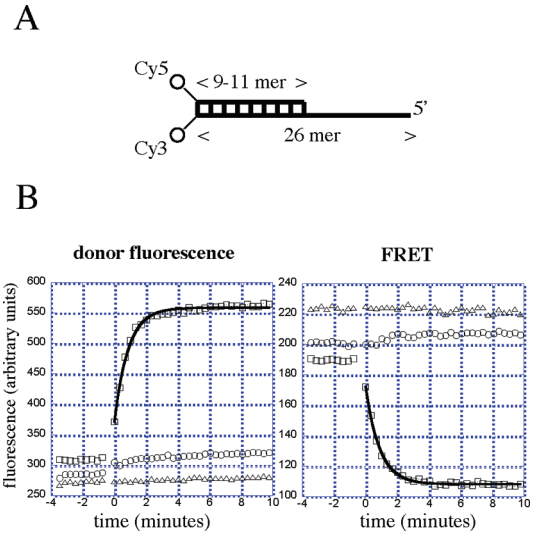

FIGURE 1: Principle of the RNA helicase assay used here. (A) Schematic representation of the substrates used. Thick bars marked < 9−11 mer > and < 26 mer > represent oligoribonucleotides that are complementary over part of their length (vertical bars). These oligonucleotides are labeled with the fluorophores Cy3 (< 26 mer >) or Cy5 (< 9−11 mer >) at their 3′ or 5′ extremities, respectively. (B) Typical time course of the Cy3 fluorescence (left) and of the Cy3 to Cy5 FRET signal (right) during the unwinding of an RNA substrate shown in panel A by a DEAD-box protein. Empty triangles or circles correspond to data for samples containing the substrate but either no helicase or no ATP, respectively, while empty squares correspond to data for a sample containing all three components. The latter values were fitted to a single-exponential curve (—) as described in the text. Protein was added at time zero. The illustrated example corresponds to the unwinding of the 9-mer/26-mer substrate by RhlE_Cp at 10 °C.

Additional Controls. In control experiments, the concentrations of DEAD-box protein and ATP in the unwinding reactions were varied over ranges of 0.3−2 μM and 1−2 mM, respectively. Similarly, for RhlE_Ec and RhlE_Cp, the concentration of the 14-mer competitor was varied over the range of 0.2−1 μM. None of these changes significantly affected unwinding rates.

To validate the unwinding assay, the results were compared to those of the conventional electrophoretic method. Assays were performed at 25 °C with a duplex consisting of the Cy3 26-mer and the Cy5 11-mer, under the same conditions described above. At timed intervals, aliquots were removed and treated as described in ref *19*. Gels were analyzed with a Typhoon Trio phosphorimager (Amersham Biosciences) in fluorescence mode (Cy5 detection): bands corresponding to the duplex were corrected from background and quantified. Data were analyzed assuming first-order kinetics and yielded k_{unw} values similar to those obtained from the fluorescence assay.

RESULTS

SrmB and RhlE Orthologs in P. haloplanktis and C. psychrerythraea. A prerequisite for this study was the availability of psychrophilic relatives of *E. coli* whose genome has been sequenced, so that orthologs of *E. coli* DEAD-box proteins can be identified. The Antarctic bacterium *P. haloplanktis* TAC125 (*35*) and the Arctic bacterium *C. psychrerythraea* 34H (*36*) were the

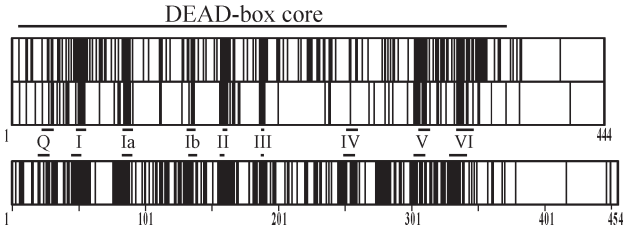

FIGURE 2: SrmB and RhlE orthologs are highly homologous to each other throughout the DEAD-box core. The top barcode shows the alignment of SrmB_Ph and SrmB_Cp on the SrmB_Ec sequence (444 amino acids) and the bottom one the alignment of RhlE_Ph and RhlE_Cp on the RhlE_Ec sequence (454 amino acids). In the middle barcode, two unrelated DEAD-box proteins (RhlE_Ec and RhlB_Ec) have been aligned on the SrmB_Ec sequence. Alignments were done with CLUSTALW, and vertical bars indicate identical residues. The horizontal bar above the panel represents the DEAD-box core of SrmB_Ec, assumed to extend from a conserved phenylalanine residue upstream of the Q motif to amino acid 368, after a predicted α-helix that is conserved in known structures of DEAD-box proteins. Small horizontal bars facing the middle and bottom barcodes show the positions of the nine DEAD-box conserved motifs in SrmB_Ec and RhlE_Ec, respectively.

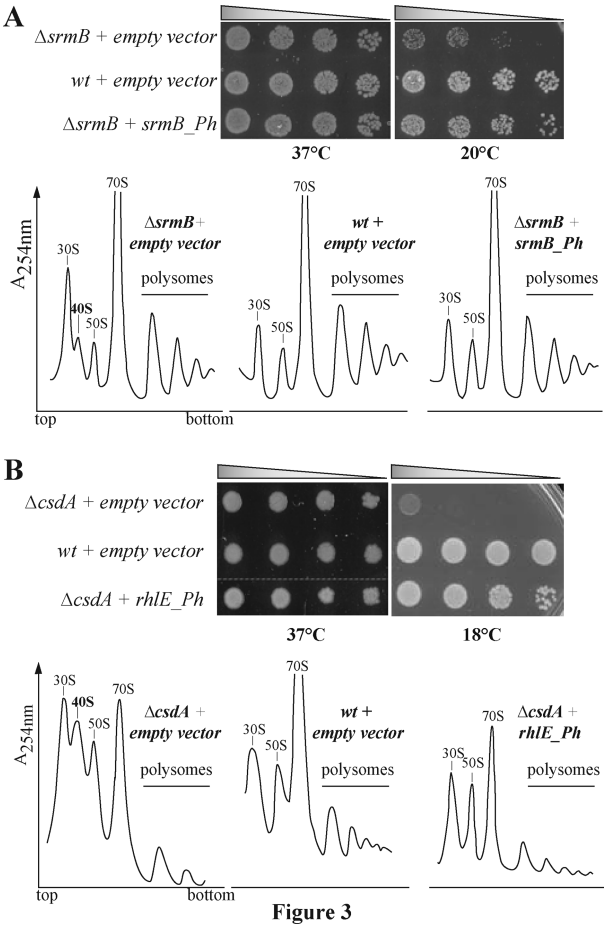

Figure 3

FIGURE 3: SrmB and RhlE orthologs from *P. haloplanktis* and *C. psycherythraea* are functionally equivalent to the *E. coli* proteins. (A) SrmB from *P. haloplanktis* (SrmB_Ph) complements the growth and ribosome assembly defect of *E. coli* cells lacking SrmB. In the top panels, growth tests on agar show that *E. coli* cells lacking SrmB (ΔSrmB) grow more slowly than their $SrmB^+$ counterparts (wt) at 20 °C, and that the expression of SrmB_Ph alleviates this defect. The bottom panel shows polysome profiles (30 °C) showing that *E. coli* cells lacking SrmB show a deficit in 50S subunits and an accumulation of a misassembled 50S-related particle (40S) (compare left and central traces), which can be corrected by expressing SrmB_Ph (rightmost trace). (B) RhlE from *P. haloplanktis* (RhlE_Ph) can complement the growth and ribosome assembly defect of *E. coli* cells lacking CsdA (DeaD). Assays were run as described for panel A, except that the RhlE_Ph gene was borne on an expression plasmid that was either not induced (growth tests) or induced only transiently (polysome profiles). For polysome profiles, cells were grown at 25 °C.

only psychrophilic γ-proteobacteria for which sequence information was available at the start of this work. Their genomes were screened with BLAST-P, using the *E. coli* DEAD-box proteins SrmB and RhlE as probes. This screen identified a number of DEAD-box proteins (9 in *P. haloplanktis* and 11 in *C. psychrerythraea*). However, for each organism, two DEAD-box proteins exhibited particularly high homology scores with respect to the two probes, and they were taken as SrmB and RhlE orthologs in these organisms. In the following, we use the suffixes _Ec (*E. coli*), _Ph (*P. haloplanktis*), and _Cp (*C. psychrerythraea*) to indicate the origin of these orthologs.

Homology between SrmB and RhlE orthologs was widespread over the DEAD-box core (ca. 360 amino acids), as shown by the distribution of the residues that are identical among all three proteins within each series; in contrast, for unrelated DEAD-box proteins, identity was largely confined to the conserved motifs (Figure 2). Pairwise comparisons showed that SrmB_Ph and SrmB_Cp proteins were slightly closer to each other (61% identical residues over the DEAD-box core) than to their *E. coli* ortholog (54−56% identity). The same trend was observed within the RhlE series (68 and 64−66% identity, respectively). Presumably, many of the differences between orthologs reflect genetic drift between different species. Yet, comparison of the psychrophilic SrmB and RhlE with their mesophilic orthologs showed a striking reduction in the Arg/Lys ratio and, in the RhlE series, a reduction in the number of charged residues and an increase in Asn content. These particular sequence biases are characteristic of psychrophilic proteins (*5*, *35*).

Complementation Studies. The psychrophilic orthologs of SrmB and RhlE were then tested for their ability to functionally replace their *E. coli* counterparts. For SrmB, we exploited the fact that *E. coli* cells lacking the corresponding gene grow slowly at a low temperature (20 °C). Moreover, these cells show a deficit in 50S ribosomal subunits and an accumulation of an imperfectly assembled subunit [40S particle (see ref *26* and Figure 3A)]. The *srmB_Ph* and *srmB_Cp* genes, together with flanking sequences including a potential promoter, were cloned into a low-copy number vector (see Experimental Procedures). When introduced into Δ*srmB E. coli* cells, the resulting plasmids restored both normal growth at 20 °C and the normal polysome profile, whereas the parent vector did not (Figure 3A; only the experiment with SrmB_Ph is shown). Thus, SrmB_Ph and SrmB_Cp are functionally equivalent to SrmB_Ec.

The *rhlE* deletion produces no obvious phenotype in *E. coli* (*17*). However, *E. coli* cells lacking the DEAD-box protein CsdA show a growth defect at 20 °C that can be alleviated via overexpression of RhlE (*17*, *25*, *29*). To prepare the RhlE_Ec, RhlE_Ph, and RhlE_Cp proteins, the corresponding genes were cloned into an expression vector under the control of an IPTG-inducible promoter (see below). We observed that, under partial induction or even without induction, the presence of these plasmids in *E. coli* cells lacking CsdA improves growth at 18 °C, whereas the parent plasmid did not. Presumably, the limited RhlE synthesis is enough to compensate, at least partially, for the absence of the *csdA* gene, and RhlE_Ph and RhlE_Cp are qualitatively equivalent to RhlE_Ec in this test. Quantitatively, growth improvement was

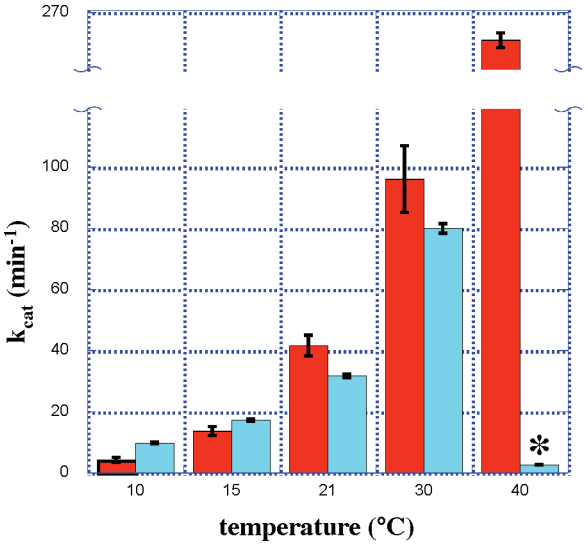

FIGURE 4: Cold adaptation of the ATPase activity of SrmB_Ph. The maximal ATPase velocities (k_{cat}) of SrmB_Ph (blue bars) and SrmB_Ec (red bars) are compared at different temperatures, using poly(A) as the RNA stimulator. SrmB_Ph is heat-labile but becomes comparatively more efficient than RhlE_Ec at low temperatures, indicating a lower activation enthalpy. At 40 °C, the activity of SrmB_Ph vanishes rapidly over time; the corresponding value (marked with an asterisk) does not correspond to the steady state, but to an average over the first few minutes of the reaction (2 min in this particular case).

more effective with RhlE_Ph (Figure 3B) than with RhlE_Cp or RhlE_Ec (not illustrated), perhaps due to differences in expression. Besides its effect on growth, the absence of CsdA also results in a defect in assembly of the 50S ribosomal subunit, as shown again by the accumulation of an incomplete 40S particle (*27*, *29*, *30*). At 25 °C, the presence of the plasmid carrying the *rhlE_Ph* gene largely corrected this defect, as judged by the disappearance of the 40S particle (Figure 3B). Again, RhlE_Ec and RhlE_Cp were less efficient in this respect (not shown). As a control, we checked that both defects are fully corrected by the presence of the same plasmid carrying the *E. coli csdA* gene (not shown).

On the basis of these tests, we conclude that the psychrophilic orthologs of SrmB and RhlE are functionally equivalent to their *E. coli* counterparts.

The ATPase Activity of Psychrophilic SrmB, but Not That of Psychrophilic RhlE, Is Cold-Adapted. The four psychrophilic proteins (SrmB_Ph, SrmB_Cp, RhlE_Ph, and RhlE_Cp), together with SrmB_Ec and RhlE_Ec, were prepared as described in Experimental Procedures. However, no meaningful enzymatic data could be obtained for SrmB_Cp. The ATPase activity of this protein exhibited large day-to-day variations, presumably reflecting its high propensity to aggregate, as judged by gel filtration analysis. Therefore, our comparison of mesophilic and psychrophilic SrmB is limited to SrmB_Ec and SrmB_Ph.

(*i*) *ATPase Activity and Heat Lability of SrmB*. The ATPase activity of most DEAD-box proteins is strongly and nonspecifically stimulated by RNA (*41*). SrmB_Ec is somewhat atypical in that its ATPase activity responds very differently to various natural or synthetic RNA species. Thus, it is well stimulated by poly(A) but not by poly(U) or *E. coli* tRNA (*19*). The same hierarchy was found with SrmB_Ph, further supporting the relatedness of the two proteins. Poly(A), which at saturating concentrations stimulated the ATPase activity of SrmB_Ec or SrmB_Ph > 20-fold, was chosen as a standard activator here.

Table 1: Comparison of the K_m Values for ATP (millimolar) of the Different DEAD-Box Proteins Used in This Study (ATPase activity)

	10 °C	25 °C
SrmB_Ec	0.02 ± 0.005	0.06 ± 0.02
SrmB_Ph	0.6 ± 0.03	0.9 ± 0.1
RhlE_Ec	0.7 ± 0.2	0.9 ± 0.3
RhlE_Cp	0.2 ± 0.04	0.2 ± 0.06
RhlE_Ph	0.3 ± 0.15	0.75 ± 0.15

The activities of the two proteins at saturating concentrations of poly(A) and ATP/Mg (i.e., the maximal velocity, or k_{cat}) were then compared (Figure 4). At 30 °C, the k_{cat} of SrmB_Ec is higher than that of SrmB_Ph, but it decreased more steeply with temperature so that SrmB_Ph becomes more active below 20 °C. This differential behavior reflects a large difference in activation enthalpy $\Delta H^{\ddagger}$, as measured from the slope of $\ln(k_{cat})$ versus $-1/RT$ (Arrhenius plot). For SrmB_Ph, this plot was linear with a slope of 17.5 kcal/mol. For SrmB_Ec, it was concave downward; however, the average slope (26.5 kcal/mol) was much higher than that for SrmB_Ph. That the two enzymes show comparable activities in the studied temperature range despite their large difference in $\Delta H^{\ddagger}$ means that the activation entropy ($\Delta S^{\ddagger}$) is also lower for the psychrophilic enzyme (see eq 1 in the Discussion for the definition of $\Delta S^{\ddagger}$). Also clearly apparent from Figure 4 is the fact that the ATPase activity of SrmB_Ph is markedly heat-labile: at 40 °C, it was rapidly inactivated, whereas SrmB_Ec remained active over time (see the legend of Figure 4).

Next, the concentrations of ATP/Mg and poly(A) were systematically varied, and the K_m values for these substrates were compared for SrmB_Ec and SrmB_Ph. In the temperature range of 10−25 °C, the K_m for ATP/Mg is 15−30-fold larger for SrmB_Ph than for SrmB_Ec (Table 1). The same trend was observed for the K_m for poly(A), although in this case the difference was smaller [< 3-fold (results not shown)].

Thus, compared to its mesophilic counterpart, the psychrophilic enzyme SrmB_Ph exhibits reduced $\Delta H^{\ddagger}$ and $\Delta S^{\ddagger}$, a larger K_m for substrates, and reduced thermal stability. All these features are hallmarks of cold adaptation (*3*−*5*).

(*ii*) *ATPase Activity and Heat Lability of RhlE*. Likewise, we compared the ATPase activities of RhlE_Ec, RhlE_Ph, and RhlE_Cp. Like for the SrmB series, all three proteins were efficiently stimulated by poly(A), which was used as the activator in most experiments. Quantitatively, at a given temperature, maximal velocities (k_{cat}) were higher for the RhlE than for the SrmB series (by 1.5−20-fold, depending upon the protein and temperature used), as previously documented with RhlE_Ec and SrmB_Ec (*19*). However, the most intriguing difference lies in the absence of cold adaptation of the ATPase activity from psychrophilic RhlEs. RhlE_Ec was slighly more active than its psychrophilic counterparts and remained so throughout the temperature range examined [5−28 °C (Figure 5)]. Consistently, Arrhenius plots yielded similar activation enthalpies for the three enzymes [from 14 (RhlE_Ec) to 15.8 (RhlE_Ph) kcal/mol]. The fact that the k_{cat} and $\Delta H^{\ddagger}$ are similar for the three enzymes means that the $\Delta S^{\ddagger}$ is also similar (eq 1). The variations in K_m for substrates within the RhlE series also did not follow the same trend as with the SrmB series. Rather, the K_m for ATP was slightly but reproducibly lower for RhlE_Cp and RhlE_Ph than for RhlE_Ec (Table 1). The only classical feature of cold-adapted enzymes exhibited by RhlE_Ph and RhlE_Cp is heat lability: like SrmB_Ph, but unlike RhlE_Ec, both proteins were rapidly inactivated at 40 °C (Figure 5).

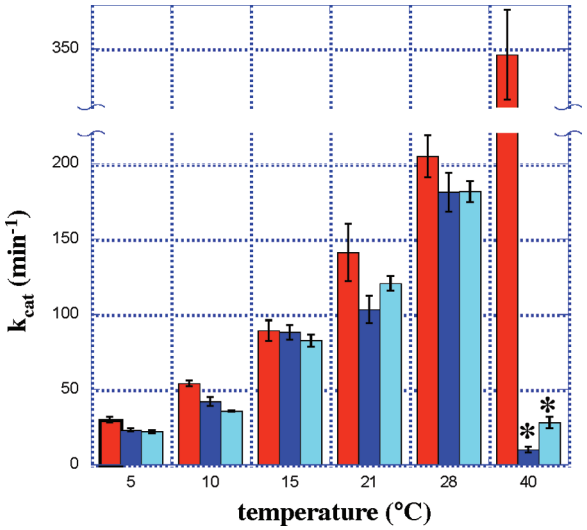

FIGURE 5: ATPase activity of psychrophilic RhlEs showing no evidence of cold adaptation. Same as Figure 4, except that RhlE_Ec (red bars), RhlE_Ph (light blue bars), and RhlE_Cp (dark blue bars) were compared. Note that whatever the temperature in the 5−28 °C range, the *E. coli* enzyme remains slightly more active than its psychrophilic counterparts. For the significance of values marked with asterisks, see the legend of Figure 4.

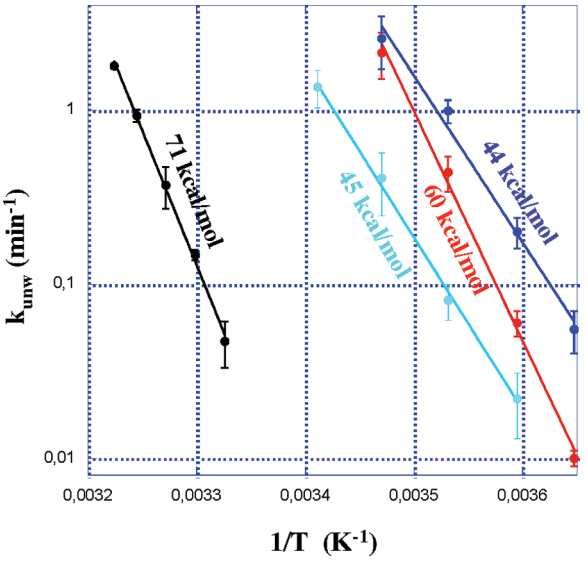

FIGURE 6: Rate constant for unwinding of a 9 bp RNA duplex as a function of temperature, in the absence of protein (black) or in the presence of RhlE_Ec, RhlE_Cp, or RhlE_Ph (red, dark blue, and light blue, respectively). The data are presented in the form of Arrhenius plots; the activation enthalpies calculated from the slope of the plots are indicated.

As a test for the robustness of these results, we turned to a different RNA activator, i.e., a 9 bp duplex with a 17 nt 5′-overhang used as a substrate for unwinding assays (see below). This RNA proved to be only slightly (ca. 1.5-fold) less efficient than poly(A) in stimulating RhlE_Ec and RhlE_Cp, but with RhlE_Ph, the decrease was more marked (5-fold). Nevertheless, the k_{cat} values of the three enzymes were again affected very similarly by temperature, and the corresponding activation enthalpies (from 13.5 to 14.5 kcal/mol) were close to those obtained with poly(A) (not illustrated).

The RNA Helicase Activity of Psychrophilic RhlE Is Cold-Adapted. (*i*) *A Fluorometric Assay for RNA Helicase Activity*. In vitro, most DEAD-box proteins possess an ATP-dependent helicase activity in addition to their ATPase activity. Since the psychrophilic RhlE exhibited no obvious adaptation of their ATPase activities to the cold, we investigated whether the same holds for the helicase activity. The classical helicase assay, involving electrophoretic analysis of aliquots taken at timed intervals during the unwinding reaction, is laborious and often inaccurate. We therefore devised an assay based on fluorescence resonance energy transfer (FRET). Similar assays have been described previously (*42*, *43*). Briefly, two complementary RNA oligonucleotides are labeled at their 3′ and 5′ ends with the two fluorophores Cy3 and Cy5, respectively. Upon formation of the duplex, FRET from Cy3 to Cy5 is observed and Cy3 fluorescence is quenched; conversely, when the samples unwind, FRET vanishes and Cy3 fluorescence increases. Both variations can be measured continuously with time, allowing accurate determination of unwinding rates (Figure 1B).

The natural substrates of RhlE are unknown, so that we had to design a model substrate. RhlE_Ec is able to unwind blunt-end duplexes, a property shared by only a few DEAD-box proteins (*19*). Preliminary experiments showed that RhlE_Cp behaves similarly but that RhlE_Ph required a single-strand extension for activity. For this reason, we designed a substrate consisting of a Cy5-labeled 9-mer annealed to a Cy3-labeled 26-mer, with a 17 nt 5′-overhang (see Experimental Procedures and Figure 1A). Moreover, a nonlabeled 14-mer RNA oligonucleotide complementary to the 9-mer was present in 10-fold excess to prevent reannealing of the separated oligonucleotides during the reaction (*19*). The presence of the competitor does not interfere with unwinding, as judged by the fact that unwinding rate is insensitive to competitor concentration. To achieve significant rates, assays were performed with a large excess of enzyme over substrate or competitor, as usual in DEAD-box proteins tested in vitro (*18*). Under these conditions, unwinding is readily observed. Controls showed that the concentrations routinely used for ATP and protein (2 mM and 0.6−0.8 μM, respectively) were sufficient to approach maximal unwinding rates (see Experimental Procedures).

(*ii*) *RhlE Orthologs: Unwinding Rates versus Temperature*. The rates of unwinding of the 9-mer substrate by RhlE_Ec, RhlE_Ph, and RhlE_Cp were then compared in the temperature range of 0−15 °C. Despite the fact that RhlE_Cp is slightly less efficient than RhlE_Ec as an ATPase (Figure 5), it was more efficient as a helicase. Moreover, the lower the temperature, the larger the difference: thus, while the unwinding activity of RhlE_Ec decreased 200-fold from 15 to 1 °C, with RhlE_Cp the decrease was only 45-fold; as a consequence, the ratio between the two activities, which is 1.2-fold at 15 °C, reaches 5.5-fold at 1 °C. The Arrhenius plots (Figure 6) reflected this difference: whereas the activation enthalpy ($\Delta H^{\ddagger}$) for RhlE_Ec was ~60 kcal/mol, for RhlE_Cp it decreased to 44 kcal/mol. As for RhlE_Ph, it was less efficient as a helicase than either RhlE_Cp or RhlE_Ec whatever the temperature (Figure 6). This result parallels ATPase assays (see above) and may indicate that the substrate used is not optimal for this particular enzyme. Nevertheless, compared to RhlE_Ec, RhlE_Ph became comparatively more efficient as the temperature decreased. Consistently, the corresponding $\Delta H^{\ddagger}$ (45 kcal/mol) is much lower than that observed with RhlE_Ec and similar to the RhlE_Cp value.

For the sake of comparison, we also measured the rate of duplex dissociation under the same conditions but in the absence of protein. Spontaneous unwinding was readily measurable in the

Table 2: Comparison of the Rate Constants [k_{unw} (min $^{-1}$)] for the Unwinding of Duplexes of Various Lengths (base pairs) by the *E. coli* (Ec) and *C. psychrerythraea* (Cp) RhlEs at 10 °C

	9 bp	10 bp	11 bp
k_{unw}			
RhlE_Ec	0.44 ± 0.1	0.03 ± 0.003	0.012 ± 0.003
RhlE_Cp	0.99 ± 0.15	0.06 ± 0.01	0.035 ± 0.01
$k_{unw}^{Cp}/k_{unw}^{Ec}$	2.25	2.0	2.9

temperature range of 27−37 °C (Figure 6). From the Arrhenius plot, the activation enthalpy was estimated to be 71 kcal/mol, which was very close to the standard enthalpy for duplex dissociation (76 kcal/mol) calculated from tabulated values using the nearest-neighbor approximation (*44*) corrected for the salt concentration used here (*45*). Extrapolation shows that, in the range of 0−15 °C, spontaneous unwinding is orders of magnitude slower than DEAD-box-mediated unwinding (Figure 6), explaining why it does not interfere with our assay (Figure 1B).

To summarize this section, the rate of duplex unwinding is considerably increased by the presence of the RhlEs, and the corresponding activation enthalpy ($\Delta H^{\ddagger}$) is decreased, as expected. However, $\Delta H^{\ddagger}$ is even lower with RhlE_Cp or RhlE_Ph than with RhlE_Ec, so that unwinding by these proteins is less temperature-dependent than with RhlE_Ec. However, compared with that of RhlE_Ec, the activities of RhlE_Cp and RhlE_Ph are not as high as predicted from the reduction in $\Delta H^{\ddagger}$, indicating that $\Delta S^{\ddagger}$ is also reduced (eq 1). These observations document the adaptation of the unwinding activities of RhlE_Cp and RhlE_Ph to low temperatures, in contrast with their ATPase activities.

(*iii*) *Unwinding Rates versus Duplex Length*. To further compare the unwinding activities of RhlE_Ec and RhlE_Cp, we investigated the influence of duplex length (and hence duplex stability) on these activities. To this end, we extended the length of the 9 bp duplex by 1 bp increments, to 10 and 11 bp (Figure 1A). Measurements were taken at 10 °C, where unwinding rates were easily measurable for both enzymes and all three duplexes. As expected, this rate decreased rapidly with duplex stability whatever the enzyme (for RhlE_Ec, the decrease was 35-fold in going from the 9-mer to the 11-mer). However, importantly, the ratio of the unwinding rates for the two enzymes varied by less than 50% in this series (Table 2). This result has implications for interpreting the cold adaptation of unwinding activity of psychrophilic RhlEs (see the Discussion).

DISCUSSION

Cold Adaptation of Enzyme Catalysis. During recent years, enzymes from psychrophilic and mesophilic origin have been extensively compared, yielding general rules for adaptation of enzyme activity to low temperatures. These rules can be conveniently summarized using the transition state theory (TST) formalism. Indeed, in most cases, the temperature dependence of the catalytic constants (k_{cat}) of enzymatic reactions follows the classical TST equation (*46*):

$$k_{cat} = (k_B \times T/h)e^{-\Delta G^{\ddagger}/RT} = (k_B \times T/h)e^{\Delta S^{\ddagger}/R}e^{-\Delta H^{\ddagger}/RT} \quad (1)$$

where k_B and h are the Boltzmann and Planck constants, respectively, $\Delta G^{\ddagger}$ (activation free energy) is the free energy difference between the transition state and the substrate state, and $\Delta H^{\ddagger}$ and $\Delta S^{\ddagger}$ are the associated activation enthalpies and entropies, respectively. Equation 1 is equivalent to the empirical Arrhenius equation [$k_{cat} = Ae^{-E_a/RT}$, where $\Delta H^{\ddagger} \sim E_a$ (activation energy) and $\Delta S^{\ddagger}$ is embedded in the pre-exponential term A].

Compared to their mesophilic counterparts, psychrophilic enzymes are generally characterized by a higher k_{cat} at low temperatures, due to a reduction in $\Delta H^{\ddagger}$ that attenuates the effect of temperature changes. However, the increase in k_{cat} is invariably smaller than expected from the reduction in $\Delta H^{\ddagger}$, which means that $\Delta S^{\ddagger}$ is also reduced (eq 1). Moreover, psychrophilic enzymes are also generally more heat-labile than their mesophilic counterparts, and their affinity for their substrates is also often reduced; i.e., K_m values are increased (for reviews, see refs (*3*−*5*)). These changes are here collectively termed "cold adaptation". It has been suggested that the decrease in $\Delta S^{\ddagger}$, the increase in K_m, and the reduced thermal stability are the price paid for a reduced $\Delta H^{\ddagger}$, which is the main adaptation of psychrophilic enzymes to low temperatures (*3*−*5*).

The generalizations described above have been based largely on studies with simple catabolic enzymes (*5*). In particular, no enzymes involved in RNA metabolism have been studied in this respect. Here, we have compared two DEAD-box proteins from *E. coli* (Ec) with their orthologs from two psychrophilic γ-proteobacteria, *P. haloplanktis* (Ph) and *C. psychrerythraea* (Cp). In vitro, these enzymes, called SrmB and RhlE, catalyze the RNA-dependent hydrolysis of ATP and the unwinding of short RNA duplexes. However, they differ considerably in this latter capacity: SrmB_Ec cannot unwind a 14-mer duplex that RhlE_Ec easily unwinds, despite the fact that the ATPase activity of both proteins is stimulated by this duplex (*19*). More generally, SrmB has been found to be orders of magnitudes less efficient than a series of other DEAD-box proteins for unwinding a 10-mer duplex (*13*).

With regard to ATPase activity, SrmB_Ph exhibits all the hallmarks of cold adaptation whereas RhlE_Ph and RhlE_Cp exhibit none, except for heat lability. In contrast, for the unwinding activity, RhlE_Ph and RhlE_Cp are clearly cold-adapted. SrmB_Ph could not be evaluated in this respect because the unwinding activity of SrmB orthologs is too low for accurate measurements versus temperature. The structural basis for these cold adaptations remains elusive and is tentatively discussed in the Supporting Information. Here, we first attempt to rationalize the fact that the unwinding activity of psychrophilic RhlEs can be cold-adapted whereas their ATPase activity is not. Next, we propose that the different modes of cold adaptation of these proteins reflect their different roles in vivo. Finally, we briefly discuss possible mechanisms whereby fast interconversion of RNA structures can be maintained at low temperatures in psychrophilic bacteria.

The ATPase and Unwinding Activities Need Not Be Correlated. The mechanism of duplex unwinding by DEAD-box proteins has been extensively studied recently (see ref *47* for a review); although several points remain unclear, what has been learned is tentatively summarized in Figure 7A. These proteins possess a "helicase core" consisting of two RecA-like domains with an ATP binding site between them (*10*, *11*, *41*). The binding of ATP on one hand and the binding of RNA on the other synergistically favor the transition from an "open" (state 1 in Figure 7A) to a "closed" conformation (state 2) in which the two RecA-like domains are brought together (*48*−*54*). Only in this conformation can ATP hydrolysis occur. The closed conformation

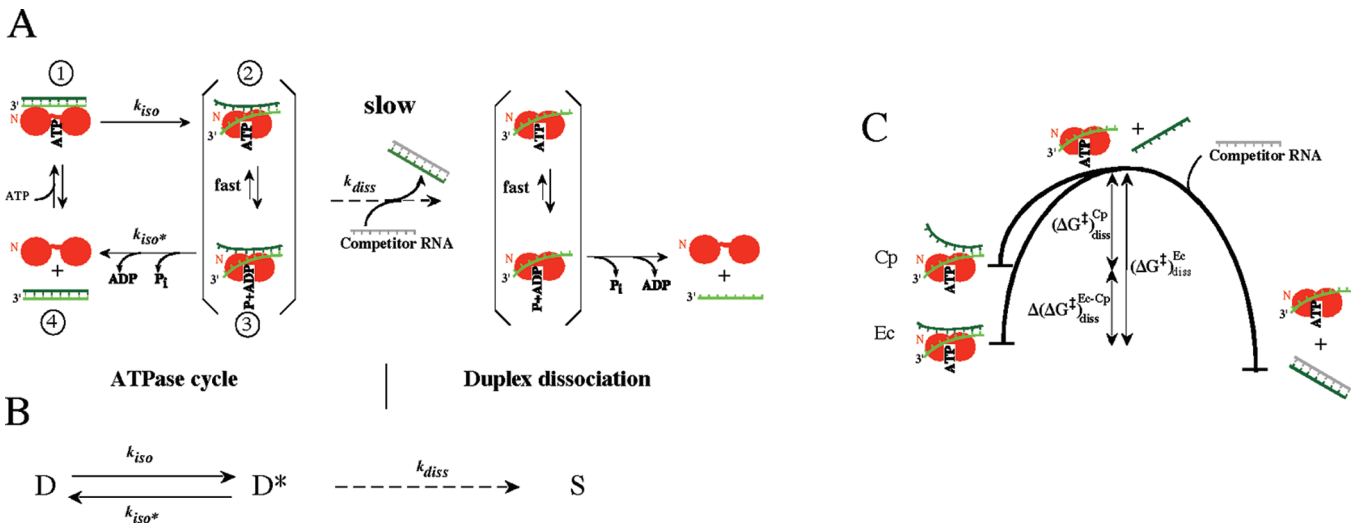

FIGURE 7: Cartoon illustrating current views of the mechanism of duplex unwinding by DEAD-box proteins, and how this activity can be cold-adapted. (A) ATPase cycle and its relation to unwinding. On their own, DEAD-box proteins adopt an open conformation in which the two RecA-like domains are loosely connected. However, in the presence of both ATP and RNA, the protein switches to a closed conformation (state 1 to state 2 transition) in which duplex RNA is partially unwound. ATP hydrolysis per se does not induce major conformational changes (state 3), but following the release of P_i and ADP, the open conformation is restored and RNA is released (state 4). The cycle is characterized by two rate-limiting steps that precede and follow ATP hydrolysis (k_{iso} and k_{iso*}, respectively). In state 2 and presumably state 3, the partially unwound duplex can occasionally dissociate (k_{diss}). The presence in the assay of excess competitor RNA (gray) makes this step irreversible by capturing the released strand (dark green). The removal of P_i and ADP then causes the enzyme to release its grip on the second strand (light green), eventually allowing multiple turnovers (*55*). (B) Under the conditions of the unwinding assay (saturating concentration of protein and ATP), scheme A simplifies into an apparent equilibrium between native duplex D and partially unwound duplex D*, with the latter occasionally dissociating (dashed arrow) into single strands (S). (C) Cartoon explaining how, by unwinding more base pairs than *E. coli* RhlE (Ec) in states 2 and 3, the RhlE from *C. psychrerythraea* (Cp) may accelerate duplex dissociation by a factor that is independent of duplex length (see the text).

binds RNA tightly but cannot accommodate a regular A helix. Consequently, duplex RNA is probably unwound over a few base pairs at this stage, which may result in complete dissociation (dashed arrow with rate constant k_{diss} in Figure 7A) if the residual duplex is sufficiently unstable (*55*, *56*). Oddly, whereas nonhydolyzable ATP analogues favor the formation of closed complexes resembling stage 2 (*53*, *57*, *58*), only some of them promote duplex dissociation (*55*), presumably due to subtle conformational differences. ATP hydrolysis (state 2 → state 3) does not appear to induce major conformational changes in itself (*53*, *57*, *58*). However, after the release of the products P_i and ADP, the protein returns to the open conformation, releasing its grip on the RNA. Duplexes that have not dissociated at this stage are free to reanneal, explaining why these enzymes can unwind only short duplexes. A detailed kinetic analysis with the *E. coli* DEAD-box protein DbpA has revealed the existence of two slow steps in the ATPase cyle (*59*): the first one precedes ATP hydrolysis and presumably corresponds to the open → closed complex isomerization, whereas the second is concomitant with P_i release and may correspond to the reverse isomerization. We refer to the corresponding rate constants as k_{iso} and k_{iso*}, respectively.

Available data show that, except for extremely weak duplexes, many futile ATPase cycles take place before the duplex eventually dissociates (*19*, *56*), which means that $k_{diss} \ll k_{iso*}$. Under the conditions used in the assay (saturating concentration of ATP and protein), the unwinding pathway then simplifies into a pre-equilibrium followed by a slow dissociation step (Figure 7B), and according to classical treatments (*46*), the unwinding rate constant becomes

$$k_{unw} = k_{diss}[k_{iso}/(k_{iso*} + k_{iso})] \quad (2)$$

Equation 2 immediately suggests why, compared with RhlE_Ec, RhlE_Cp and RhlE_Ph can be cold-adapted from the viewpoint of unwinding activity even though all three proteins show comparable ATPase activities (i.e., comparable k_{iso*} and k_{iso} values) whatever the temperature (Figures 5 and 6). Simply, it is the dissociation of the partially unwound duplex, characterized by k_{diss}, that must be cold-adapted. Though more complicated interpretations exist, we speculate that the psychrophilic RhlEs can unwind more base pairs than RhlE_Ec in the closed conformation (states 2 and 3 in Figure 7A). Fewer base pairs then remain to be broken during dissociation (Figure 7C), which means a reduced $\Delta H^{\ddagger}_{diss}$ and hence a reduced $\Delta H^{\ddagger}_{unw}$, as indeed observed. From the reduction in $\Delta H^{\ddagger}_{unw}$ (from 60 kcal/mol for RhlE_Ec to 44−45 kcal/mol for RhlE_Cp or RhlE_Ph), we can estimate from nearest-neighbor parameters that one or two extra base pairs are unwound by the psychrophilic RhlEs in the closed conformation (*44*). That RhlE_Cp unwinds more base pairs than RhlE_Ec is consistent with the fact that the ratio of their unwinding rates, i.e., $k^{Cp}_{unw}/k^{Ec}_{unw}$, is insensitive to duplex length (Table 2). Indeed, assuming that k_{iso*} and k_{iso} are the same for both proteins, eqs 1 and 2 show that

$$k^{Cp}_{unw}/k^{Ec}_{unw} = k^{Cp}_{diss}/k^{Ec}_{diss} = e^{-(\Delta G^{\ddagger})^{Cp}_{diss}/RT}/e^{-(\Delta G^{\ddagger})^{Ec}_{diss}/RT}$$

$$= e^{-\Delta(\Delta G^{\ddagger})^{Cp-Ec}_{diss}/RT}$$

In this expression, $-\Delta(\Delta G^{\ddagger})^{Cp-Ec}_{diss}$ is the free energy cost for the opening of extra base pairs by RhlE_Cp (Figure 7C). This cost and, therefore, $k^{Cp}_{unw}/k^{Ec}_{unw}$ should depend upon only the number of these extra base pairs and not upon the length of the duplex, as indeed observed.

In summary, using available information, one can rationalize the fact that the unwinding activity of psychrophilic RhlEs is cold-adapted whereas their ATPase activity is not. More generally, it is clear from eq 2 that, when different DEAD-box proteins are compared, no systematic correlation is expected between the rates of the ATPase and unwinding reactions.

For instance, increasing k_{iso*}, which corresponds to the slowest of the two slow steps in the DbpA ATPase cycle (*59*), will in fact *decrease* the unwinding rate by shortening the lifespan of the closed conformation, an obligate intermediate toward dissociation (Figure 7A,B).

Cold Adaptation versus Biological Function of RhlE and SrmB. It seems plausible that the cold adaptation of an enzymatic activity reflects its importance in vivo. As discussed above, DEAD-box proteins possess two distinct activities, RNA unwinding and RNA-dependent ATPase. The unwinding activity of psychrophilic RhlE is cold-adapted, suggesting that this activity is physiologically relevant. In contrast, in the case of SrmB_Ph, it is the ATPase activity that is cold-adapted and thus presumably important. The limited information available on the role of these two proteins is consistent with these views.

RhlE orthologs are widespread in bacteria (*17*). In the psychrophilic organism *Pseudomonas syringae*, RhlE assembles with RNase E and the exonuclease RNase R into a "degradosome", much as RhlB does with RNase E and the exonuclease PNPase in *E. coli* (*60*). In vitro assays show that within the *E. coli* degradosome, RhlB assists the activity of PNPase by unwinding secondary structures (*22*). It is thus likely that RhlE plays the same essential role in *P. syringae*. In *E. coli*, the removal of RhlE_Ec has no known phenotype, and its possible partners are unknown. However, when overexpressed, RhlE can substitute for CdsA (Figure 3B), another *E. coli* DEAD-box protein that has been more extensively studied. CsdA is implicated in both mRNA decay and ribosome assembly, with the former role being presumably more crucial to the cell (*17*, *25*, *29*). At low temperatures in vivo, CsdA associates with PNPase and RNase E to form a "cold-shock degradosome" (*23*), and it is required for the fast decay of at least some mRNAs (*25*). A CsdA variant mutated in the second residue of the DEAD motif, which lacks unwinding activity (*61*), is ineffective in this respect (*25*). In vitro, both CsdA and RhlE_Ec can replace RhlB in the degradosome, assisting PNPase digestion of structured RNA fragments (*23*, *62*). The functional equivalence of CsdA and RhlE_Ec suggests that, under yet undefined conditions, RhlE_Ec may also participate in the degradosome in *E. coli*, as in *P. syringae*, and help unwind mRNA secondary structures. Thus, unwinding is presumably a physiologically relevant activity for RhlE, explaining its cold adaptation in psychrophilic enzymes.

The in vivo function of SrmB is also still elusive. This protein, which assists an early step in the assembly of the 50S ribosomal subunit, forms a ribonucleoproteic complex with r-proteins L4 and L24, and their binding site near the 5′-end of 23S rRNA (*26*, *63*). Recently, the analysis of rRNA mutations that can bypass the SrmB requirement led us to hypothesize that SrmB serves to prevent spurious pairings between the nascent 50S subunit and decaying rRNA fragments (F. Proux, M. Dreyfus, and I. Iost, manuscript in preparation). While SrmB could do so either by unwinding these pairings or by acting as an ATP-dependent placeholder, as does eIF4AIII in the exon−junction complex (*49*, *50*), the weakness of the unwinding activity of SrmB argues in favor of the latter hypothesis. The ATPase activity, by allowing the protein to release its grip on the RNA, would adjust the duration of this grip to the kinetics of ribosome assembly. The cold adaptation of this activity in SrmB_Ph would simply reflect the faster assembly of the *P. haloplanktis* ribosome in the cold as compared with the *E. coli* ribosome.

Unwinding RNA in the Cold. In rich medium, *C. psychrerythraea* grows as fast at 0 °C as *E. coli* at 10 °C, yet RNA structures are considerably more stable at the former temperature. This can be illustrated with our 9-mer model duplex, whose stability falls in the upper range of hairpin stabilities in natural RNAs. Extrapolation of the data from Figure 6 shows that spontaneous unwinding of this duplex occurs 100-fold slower at 0 °C than at 10 °C. However, if we now consider that unwinding at 10 °C takes place in the presence of RhlE_Ec whereas at 0 °C it takes place in the presence of the more active RhlE_Cp, the ratio drops to only 10 (Figure 6). Another factor that is likely to favor rearrangement of RNA structures is the GC%, which is ~40% in *C. psychrerythraea* versus 50% in *E. coli*. Decreasing the GC% of the 9-mer duplex by ca. 10% by changing one GC base pair into an AU base pair decreases the free energy of the duplex by an average of 1.5 kcal/mol at 0 °C, or a factor of ~15 in stability (*44*). Another factor that may facilitate duplex dissociation in *C. psychrerythraea* is the presence of cold-shock RNA chaperones like CspA: this protein has been found to be constitutively expressed in another psychrophilic bacterium, *Arthrobacter globiformis*, when growing in the cold (*64*). Thus, psychrophilic organisms may use multiple strategies to facilitate RNA rearrangements in the cold. Presumably, these strategies are efficient: for instance, we have found that bulk mRNA decay, which requires mRNA to be single-stranded, is 4−6-fold faster in *C. psychrerythraea* than in *E. coli* at 12 °C (G. Cartier and M. Dreyfus, manuscript in preparation).

ACKNOWLEDGMENT

We thank Dr. A. Danchin for the gift of *P. haloplanktis* strain TAC125, Drs. N. K. Tanner and I. Iost for critical review of the manuscript, and Drs. J. Banroques and A. J. Carpousis for helpful discussions. We are indebted to I. Iost for the initial cloning of *P. haloplanktis* DEAD-box proteins and to Frédéric Loussala, Mélanie Béraud, and Marion Beaulieu for their participation in some experiments.

SUPPORTING INFORMATION AVAILABLE

Discussion of the structural basis for cold adaptation of the DEAD-box proteins studied here and additional experimental details. This material is available free of charge via the Internet at http://pubs.acs.org.

REFERENCES

1. Deming, J. W. (2002) Psychrophiles and polar regions. *Curr. Opin. Microbiol. 5*, 301–309.
2. D'Amico, S., Collins, T., Marx, J. C., Feller, G., and Gerday, C. (2006) Psychrophilic microorganisms: Challenges for life. *EMBO Rep. 7*, 385–389.
3. Feller, G., and Gerday, C. (2003) Psychrophilic enzymes: Hot topics in cold adaptation. *Nat. Rev. Microbiol. 1*, 200–208.
4. Georlette, D., Blaise, V., Collins, T., D'Amico, S., Gratia, E., Hoyoux, A., Marx, J. C., Sonan, G., Feller, G., and Gerday, C. (2004) Some like it cold: Biocatalysis at low temperatures. *FEMS Microbiol. Rev. 28*, 25–42.
5. Siddiqui, K. S., and Cavicchioli, R. (2006) Cold-adapted enzymes. *Annu. Rev. Biochem. 75*, 403–433.
6. Kos, M., and Tollervey, D. (2005) The Putative RNA Helicase Dbp4p Is Required for Release of the U14 snoRNA from Preribosomes in *Saccharomyces cerevisiae*. *Mol. Cell 20*, 53–64.
7. Mohr, S., Stryker, J. M., and Lambowitz, A. M. (2002) A DEAD-box protein functions as an ATP-dependent RNA chaperone in group I intron splicing. *Cell 109*, 769–779.
8. Freier, S. M., Kierzek, R., Jaeger, J. A., Sugimoto, N., Caruthers, M. H., Neilson, T., and Turner, D. H. (1986) Improved free-energy parameters for predictions of RNA duplex stability. *Proc. Natl. Acad. Sci. U.S.A. 83*, 9373–9377.

9. Turner, D. H., Sugimoto, N., and Freier, S. M. (1988) RNA structure prediction. *Annu. Rev. Biophys. Biophys. Chem. 17*, 167–192.
10. Cordin, O., Banroques, J., Tanner, N. K., and Linder, P. (2006) The DEAD-box protein family of RNA helicases. *Gene 367*, 17–37.
11. Pyle, A. M. (2008) Translocation and unwinding mechanisms of RNA and DNA helicases. *Annu. Rev. Biophys. 37*, 317–336.
12. Del Campo, M., Tijerina, P., Bhaskaran, H., Mohr, S., Yang, Q., Jankowsky, E., Russell, R., and Lambowitz, A. M. (2007) Do DEAD-box proteins promote group II intron splicing without unwinding RNA? *Mol. Cell 28*, 159–166.
13. Del Campo, M., Mohr, S., Jiang, Y., Jia, H., Jankowsky, E., and Lambowitz, A. M. (2009) Unwinding by Local Strand Separation Is Critical for the Function of DEAD-Box Proteins as RNA Chaperones. *J. Mol. Biol. 389*, 674–693.
14. Fairman, M. E., Maroney, P. A., Wang, W., Bowers, H. A., Gollnick, P., Nilsen, T. W., and Jankowsky, E. (2004) Protein displacement by DExH/D "RNA helicases" without duplex unwinding. *Science 304*, 730–734.
15. Jankowsky, E., and Bowers, H. (2006) Remodeling of ribonucleoprotein complexes with DExH/D RNA helicases. *Nucleic Acids Res. 34*, 4181–4188.
16. Ballut, L., Marchadier, B., Baguet, A., Tomasetto, C., Seraphin, B., and Le Hir, H. (2005) The exon junction core complex is locked onto RNA by inhibition of eIF4AIII ATPase activity. *Nat. Struct. Mol. Biol. 12*, 861–869.
17. Iost, I., and Dreyfus, M. (2006) DEAD-box RNA helicases in *Escherichia coli*. *Nucleic Acids Res. 34*, 4189–4197.
18. Diges, C. M., and Uhlenbeck, O. C. (2001) *Escherichia coli* DbpA is an RNA helicase that requires hairpin 92 of 23S rRNA. *EMBO J. 20*, 5503–5512.
19. Bizebard, T., Ferlenghi, I., Iost, I., and Dreyfus, M. (2004) Studies on three *E. coli* DEAD-box helicases point to an unwinding mechanism different from that of model DNA helicases. *Biochemistry 43*, 7857–7866.
20. Chandran, V., Poljak, L., Vanzo, N. F., Leroy, A., Miguel, R. N., Fernandez-Recio, J., Parkinson, J., Burns, C., Carpousis, A. J., and Luisi, B. F. (2007) Recognition and cooperation between the ATP-dependent RNA helicase RhlB and ribonuclease RNase E. *J. Mol. Biol. 367*, 113–132.
21. Iost, I., and Dreyfus, M. (1994) mRNAs can be stabilized by DEAD-box proteins. *Nature 372*, 193–196.
22. Py, B., Higgins, C. F., Krisch, H. M., and Carpousis, A. J. (1996) A DEAD-box RNA helicase in the *Escherichia coli* RNA degradosome. *Nature 381*, 169–172.
23. Prud'homme-Genereux, A., Beran, R. K., Iost, I., Ramey, C. S., Mackie, G. A., and Simons, R. W. (2004) Physical and functional interactions among RNase E, polynucleotide phosphorylase and the cold-shock protein, CsdA: Evidence for a 'cold shock degradosome'. *Mol. Microbiol. 54*, 1409–1421.
24. Khemici, V., Poljak, L., Toesca, I., and Carpousis, A. J. (2005) Evidence in vivo that the DEAD-box RNA helicase RhlB facilitates the degradation of ribosome-free mRNA by RNase E. *Proc. Natl. Acad. Sci. U.S.A. 102*, 6913–6918.
25. Awano, N., Xu, C., Ke, H., Inoue, K., Inouye, M., and Phadtare, S. (2007) Complementation analysis of the cold-sensitive phenotype of the *Escherichia coli* csdA deletion strain. *J. Bacteriol. 189*, 5808–5815.
26. Charollais, J., Pflieger, D., Vinh, J., Dreyfus, M., and Iost, I. (2003) The DEAD-box RNA helicase SrmB is involved in the assembly of 50S ribosomal subunits in *Escherichia coli*. *Mol. Microbiol. 48*, 1253–1265.
27. Charollais, J., Dreyfus, M., and Iost, I. (2004) CsdA, a cold-shock RNA helicase from *Escherichia coli*, is involved in the biogenesis of 50S ribosomal subunit. *Nucleic Acids Res. 32*, 2751–2759.
28. Elles, L. M., and Uhlenbeck, O. C. (2008) Mutation of the arginine finger in the active site of *Escherichia coli* DbpA abolishes ATPase and helicase activity and confers a dominant slow growth phenotype. *Nucleic Acids Res. 36*, 41–50.
29. Jain, C. (2008) The *E. coli* RhlE RNA helicase regulates the function of related RNA helicases during ribosome assembly. *RNA 14*, 381–389.
30. Peil, L., Virumae, K., and Remme, J. (2008) Ribosome assembly in *Escherichia coli* strains lacking the RNA helicase DeaD/CsdA or DbpA. *FEBS J. 275*, 3772–3782.
31. Sharpe Elles, L. M., Sykes, M. T., Williamson, J. R., and Uhlenbeck, O. C. (2009) A dominant negative mutant of the *E. coli* RNA helicase DbpA blocks assembly of the 50S ribosomal subunit. *Nucleic Acids Res. 37*, 6503–6514.
32. Jones, P. G., Mitta, M., Kim, Y., Jiang, W., and Inouye, M. (1996) Cold shock induces a major ribosomal-associated protein that unwinds double-stranded RNA in *Escherichia coli*. *Proc. Natl. Acad. Sci. U.S.A. 93*, 76–80.
33. Chamot, D., Magee, W. C., Yu, E., and Owttrim, G. W. (1999) A cold shock-induced cyanobacterial RNA helicase. *J. Bacteriol. 181*, 1728–1732.
34. Lim, J., Thomas, T., and Cavicchioli, R. (2000) Low temperature regulated DEAD-box RNA helicase from the Antarctic archaeon, *Methanococcoides burtonii*. *J. Mol. Biol. 297*, 553–567.
35. Medigue, C., Krin, E., Pascal, G., Barbe, V., Bernsel, A., Bertin, P. N., Cheung, F., Cruveiller, S., D'Amico, S., Duilio, A., Fang, G., Feller, G., Ho, C., Mangenot, S., Marino, G., Nilsson, J., Parrilli, E., Rocha, E. P., Rouy, Z., Sekowska, A., Tutino, M. L., Vallenet, D., von Heijne, G., and Danchin, A. (2005) Coping with cold: The genome of the versatile marine Antarctica bacterium *Pseudoalteromonas haloplanktis* TAC125. *Genome Res. 15*, 1325–1335.
36. Methe, B. A., Nelson, K. E., Deming, J. W., Momen, B., Melamud, E., Zhang, X., Moult, J., Madupu, R., Nelson, W. C., Dodson, R. J., Brinkac, L. M., Daugherty, S. C., Durkin, A. S., DeBoy, R. T., Kolonay, J. F., Sullivan, S. A., Zhou, L., Davidsen, T. M., Wu, M., Huston, A. L., Lewis, M., Weaver, B., Weidman, J. F., Khouri, H., Utterback, T. R., Feldblyum, T. V., and Fraser, C. M. (2005) The psychrophilic lifestyle as revealed by the genome sequence of *Colwellia psychrerythraea* 34H through genomic and proteomic analyses. *Proc. Natl. Acad. Sci. U.S.A. 102*, 10913–10918.
37. Wilson, K. (2001) Preparation of genomic DNA from bacteria. *Curr. Protoc. Mol. Biol.* Chapter 2, Unit 2.4.
38. Moore, J. T., Uppal, A., Maley, F., and Maley, G. F. (1993) Overcoming inclusion body formation in a high-level expression system. *Protein Expression Purif. 4*, 160–163.
39. Lerner, C. G., and Inouye, M. (1990) Low copy number plasmids for regulated low-level expression of cloned genes in *Escherichia coli* with blue/white insert screening capability. *Nucleic Acids Res. 18*, 4631.
40. Lopez, P. J., Iost, I., and Dreyfus, M. (1994) The use of a tRNA as a transcriptional reporter: The T7 late promoter is extremely efficient in *Escherichia coli* but its transcripts are poorly expressed. *Nucleic Acids Res. 22*, 1186–1193.
41. Tanner, N. K., and Linder, P. (2001) DExD/H box RNA helicases: From generic motors to specific dissociation functions. *Mol. Cell 8*, 251–262.
42. Bjornson, K. P., Amaratunga, M., Moore, K. J., and Lohman, T. M. (1994) Single-turnover kinetics of helicase-catalyzed DNA unwinding monitored continuously by fluorescence energy transfer. *Biochemistry 33*, 14306–14316.
43. Rajkowitsch, L., and Schroeder, R. (2007) Dissecting RNA chaperone activity. *RNA 13*, 2053–2060.
44. Markham, N. R., and Zuker, M. (2005) DINAMelt web server for nucleic acid melting prediction. *Nucleic Acids Res. 33*, W577–W581.
45. SantaLucia, J., Jr. (1998) A unified view of polymer, dumbbell, and oligonucleotide DNA nearest-neighbor thermodynamics. *Proc. Natl. Acad. Sci. U.S.A. 95*, 1460–1465.
46. Fersht, A. R. (1985) Enzyme Structure and Mechanism, 2nd ed., W. H. Freeman and Co., New York.
47. Hilbert, M., Karow, A. R., and Klostermeier, D. (2009) The mechanism of ATP-dependent RNA unwinding by DEAD box proteins. *Biol Chem. 390*, 1237–1250.
48. Sengoku, T., Nureki, O., Nakamura, A., Kobayashi, S., and Yokoyama, S. (2006) Structural Basis for RNA Unwinding by the DEAD-Box Protein Drosophila Vasa. *Cell 125*, 287–300.
49. Andersen, C. B., Ballut, L., Johansen, J. S., Chamieh, H., Nielsen, K. H., Oliveira, C. L., Pedersen, J. S., Seraphin, B., Le Hir, H., and Andersen, G. R. (2006) Structure of the exon junction core complex with a trapped DEAD-box ATPase bound to RNA. *Science 313*, 1968–1972.
50. Bono, F., Ebert, J., Lorentzen, E., and Conti, E. (2006) The crystal structure of the exon junction complex reveals how it maintains a stable grip on mRNA. *Cell 126*, 713–725.
51. Collins, R., Karlberg, T., Lehtio, L., Schutz, P., van den Berg, S., Dahlgren, L. G., Hammarstrom, M., Weigelt, J., and Schuler, H. (2009) The DEXD/H-box RNA helicase DDX19 is regulated by an α-helical switch. *J. Biol. Chem. 284*, 10296–10300.
52. von Moeller, H., Basquin, C., and Conti, E. (2009) The mRNA export protein DBP5 binds RNA and the cytoplasmic nucleoporin NUP214 in a mutually exclusive manner. *Nat. Struct. Mol. Biol. 16*, 247–254.
53. Del Campo, M., and Lambowitz, A. M. (2009) Structure of the Yeast DEAD box protein Mss116p reveals two wedges that crimp RNA. *Mol. Cell 35*, 598–609.

54. Theissen, B., Karow, A. R., Kohler, J., Gubaev, A., and Klostermeier, D. (2008) Cooperative binding of ATP and RNA induces a closed conformation in a DEAD box RNA helicase. *Proc. Natl. Acad. Sci. U.S.A. 105*, 548–553.
55. Liu, F., Putnam, A., and Jankowsky, E. (2008) ATP hydrolysis is required for DEAD-box protein recycling but not for duplex unwinding. *Proc. Natl. Acad. Sci. U.S.A. 105*, 20209–20214.
56. Chen, Y., Potratz, J. P., Tijerina, P., Del Campo, M., Lambowitz, A. M., and Russell, R. (2008) DEAD-box proteins can completely separate an RNA duplex using a single ATP. *Proc. Natl. Acad. Sci. U.S.A. 105*, 20203–20208.
57. Nielsen, K. H., Chamieh, H., Andersen, C. B., Fredslund, F., Hamborg, K., Le Hir, H., and Andersen, G. R. (2009) Mechanism of ATP turnover inhibition in the EJC. *RNA 15*, 67–75.
58. Aregger, R., and Klostermeier, D. (2009) The DEAD box helicase YxiN maintains a closed conformation during ATP hydrolysis. *Biochemistry 48*, 10679–10681.
59. Henn, A., Cao, W., Hackney, D. D., and De La Cruz, E. M. (2008) The ATPase cycle mechanism of the DEAD-box rRNA helicase, DbpA. *J. Mol. Biol. 377*, 193–205.
60. Purusharth, R. I., Klein, F., Sulthana, S., Jager, S., Jagannadham, M. V., Evguenieva-Hackenberg, E., Ray, M. K., and Klug, G. (2005) Exoribonuclease R interacts with endoribonuclease E and an RNA helicase in the psychrotrophic bacterium *Pseudomonas syringae* Lz4W. *J. Biol. Chem. 280*, 14572–14578.
61. Turner, A. M., Love, C. F., Alexander, R. W., and Jones, P. G. (2007) Mutational analysis of the *Escherichia coli* DEAD box protein CsdA. *J. Bacteriol. 189*, 2769–2776.
62. Khemici, V., Toesca, I., Poljak, L., Vanzo, N. F., and Carpousis, A. J. (2004) The RNase E of *Escherichia coli* has at least two binding sites for DEAD-box RNA helicases: Functional replacement of RhlB by RhlE. *Mol. Microbiol. 54*, 1422–1430.
63. Trubetskoy, D., Proux, F., Allemand, F., Dreyfus, M., and Iost, I. (2009) SrmB, a DEAD-box helicase involved in *Escherichia coli* ribosome assembly, is specifically targeted to 23S rRNA in vivo. *Nucleic Acids Res. 37*, 6540–6549.
64. Berger, F., Morellet, N., Menu, F., and Potier, P.(1996) Cold shock and cold acclimation proteins in the psychrotrophic bacterium *Arthrobacter globiformis* SI55. *J. Bacteriol. 178*, 2999–3007.